



Customized 3D-printed occluders enabling the reproduction of consistent and stable heart failure in swine models

Han B. Kim¹ · Seungman Jung² · Hyukjin Park¹ · Doo S. Sim¹ · Munki Kim¹ · Sanskrita Das³ · Youngkeun Ahn¹ · Myung H. Jeong¹ · Jinah Jang^{2,3,4}  · Young J. Hong¹

Received: 1 December 2020 / Accepted: 9 June 2021 / Published online: 2 July 2021
© Zhejiang University Press 2021

Abstract

Reproducibility of clinical output is important when investigating therapeutic efficacy in pre-clinical animal studies. Due to its physiological relevance, a swine myocardial infarction (MI) model has been widely used to evaluate the effectiveness of stem cells or tissue-engineered constructs for ischemic heart diseases. Several methods are used to induce MI in the swine model. However, it is difficult, using these approaches, to obtain a similar level of functional outcomes from a group of animals due to interpersonal variation, leading to increased experimental cost. Hence, in order to minimize human intervention, we developed an approach to use a customized occluder that has dimensional similarities with that of the coronary artery of animals in the case of the swine model. We carried out angiography to measure the diameter of the middle left anterior descending artery of each individual animal to fabricate the customized occluder using a 3D-printing system. The fabricated occluder contained a central hole smaller than that of the targeted middle left anterior descending artery to mimic an atherosclerotic coronary artery that has an approximately 20% blocked condition. Interestingly, the 3D-printed occluder can provide continuous blood flow through the central pore, indicating a high survival rate (88%) of up to 28 days post-operation. This method showed the possibility of creating consistent myocardial infarction induction as compared to the conventional representative closed-chest method (50% survival rate), thus highlighting how our method can have a profound effect on accelerating reliable experiments for developing new therapeutic approaches to ischemic heart diseases.

Han B. Kim and Seungman Jung have contributed equally to this work.

✉ Jinah Jang
jinahjang@postech.ac.kr

✉ Young J. Hong
hyj200@hanmail.net

¹ Division of Cardiology, Chonnam National University Medical School, Gwangju, Republic of Korea

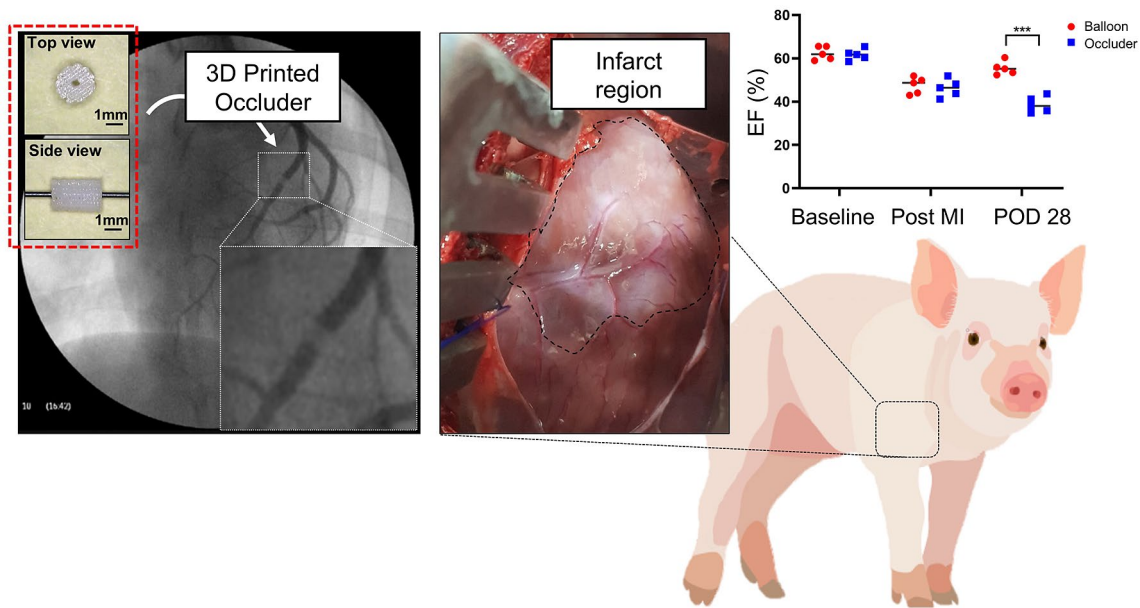
² School of Interdisciplinary Bioscience and Bioengineering, Pohang University of Science and Technology, Pohang, Republic of Korea

³ Department of Creative IT Engineering, Pohang University of Science and Technology, Pohang, Republic of Korea

⁴ Department of Mechanical Engineering, Pohang University of Science and Technology, Pohang, Republic of Korea

Graphic abstract

Customized 3D occluders for creating consistent and stable HF models



Keywords 3D bioprinting · Myocardial infarction · Ischemic heart failure · Swine model · Left anterior descending artery

Introduction

Myocardial infarction (MI) is globally recognized as a major cause of mortality and morbidity [1, 2]. In brief, MI involves the occlusion of coronary arteries, resulting in the attenuation of blood circulation to distal heart muscles and creating a hypoxic environment within the myocardium. As a result, nutritional insufficiency occurs in the myocardium, leading to myocardial necrosis and a loss of cardiac functions. In order to determine novel therapeutics for the treatment of ischemic heart diseases, various animal models play a critical role in investigating mechanistic and systemic responses *in vivo*.

Although small rodents (e.g., mice or rats) can provide significant information at the molecular level, larger animal models need to be considered when overcoming challenges in understanding the function, anatomy, and physiology of diseases at a clinical level. Among large animal models, swine have been widely used to study the pathogenesis and treatment of MI due to their similarity to humans in physiology, anatomical structure, blood lipids, hypertrophic lesions, and lipoprotein metabolism [3]. Various methods (e.g., open-chest surgical ligation, closed-chest percutaneous catheterization, and chronic total occlusion by artificial plaque) are employed to induce MI in swine models [4, 5].

However, each of these is accompanied by serious concerns regarding increased mortality due to ventricular fibrillation and ventricular tachycardia, severe infections, pericarditis, vascular calcification, and inflammation during the surgical treatment [6, 7]. Because of cost and practical efficiency, young swine are preferred as typical standard animals for MI models, given that there exists a bottleneck that induces fast infarct recovery by collateral artery regeneration [8–11].

Recently, the fabrication of custom-made and anatomically relevant structures using 3D-printing technology has been suggested as a new paradigm for medical prosthesis and grafts. This approach usually utilizes medical images (e.g., computerized tomography, magnetic resonance imaging, angiography) to facilitate computer modeling and to create a G-code to develop on-demand and complex structures with precise dimensional control [12, 13]. In this study, we designed a customized 3D-printed occluder to mimic a narrowed internal diameter of the coronary artery—induced by atherosclerosis—and applied this occluder to create an animal myocardial infarction model. In addition, we used an extrusion-based 3D-printing method to fabricate the occluder with a hole at the center to investigate the effectiveness of size on blocking blood flow. By modulating printing parameters, we could achieve high structural versatility to fabricate occluders with various dimensions of the outer

diameter and inner hole diameter, thereby creating consistent and stable MI in swine models.

Materials and methods

All animal experiments were approved by the Ethics Committee of Chonnam National University Medical School and Chonnam National University Hospital (CNU IACUC-H-2017-63), Republic of Korea. A series of timelines were strictly followed to evaluate physiological and functional changes. Balloon, a representative conventional closed-chest method to induce MI in swine model, was selected as a control group (Fig. 1).

3D-printing of the occluder

To fabricate the occluder, we selected polycaprolactone (PCL; MW 43,000, Polyscience Inc., Taiwan, China) because it is a Food and Drug Administration-approved, biocompatible and biodegradable thermoplastic material. A 3D-bioprinting system (3DXPrinter, T&R Biofab, Republic of Korea) equipped with multiple extrusion-based printing heads was used to fabricate the occluder. The PCL was loaded into a 10-cc metal syringe and was heated to 70 °C to reach its melting point, thereby allowing its extrusion (Fig. 2a). The molten PCL was extruded through a metal needle (nozzle diameter: 150 µm) on a substrate maintained at 18 °C in a layer-by-layer method as per the programmed code using a pneumatic pressure of 550 kPa and a deposition speed of 60 mm/min. Subsequent layers were deposited at an angle of 90° to the underlying layer to fabricate the occluder with structural integrity and reproducibility. The central inner hole was designed to mimic the narrow diameter of an atherosclerotic coronary artery, with an approximately 20% smaller inner diameter compared to healthy vessels. The

customized occluder was fabricated based on measurements obtained for the luminal size of the left anterior descending (LAD) artery using an angiographic system.

Preparation of swine

Yorkshire×Landrace F1 crossbred castrated male swine (20–25 kg; *n* = 22) were randomly allocated. Of these, 19 swine were divided into two groups: the balloon and occluder groups, and the remaining three were selected as the sham treatment group. Aspirin (100 mg/day) and clopidogrel (75 mg/day) were administered as pre-treatment three days prior to surgery. On the day of the surgery, all swine were anesthetized with zolazepam-tiletamine (2.5 mg/kg; Virbac, France), xylazine (3 mg/kg; Bayer AG, Germany), and azaperone (6 mg/kg; Janssen-Cilag, Germany). A rebreathing circle system (Multiplus MEVD Anesthesia Machine; Royal Medical, Republic of Korea) was used to maintain stable breathing during the surgical procedure. All animals were sacrificed via intravenous injection of potassium chloride post-anesthesia for the required characterization at a defined time period.

Quantitative coronary angiography

Based on angiography, the luminal diameter of the LAD artery was measured through a cardiovascular angiographic analysis system (CAAS, version 7.0, Pie Medical BV, Maastricht, the Netherland) for evaluating LAD luminal diameter.

Induction of MI using a conventional method (balloon)

To induce MI using a closed-chest method, the left carotid artery (LCA) was surgically exposed, and a 7-F introducer sheath was placed near the incision site. After the infusion of 10,000 units of heparin, a 7-F guiding catheter was placed

Fig. 1 Flowchart showing experimental timelines of functional assessments for inducing myocardial infarction. Representative experimental timelines comparing a group using a closed-chest method utilizing a balloon catheter (balloon), and a 3D-printed occluder (occluder) group

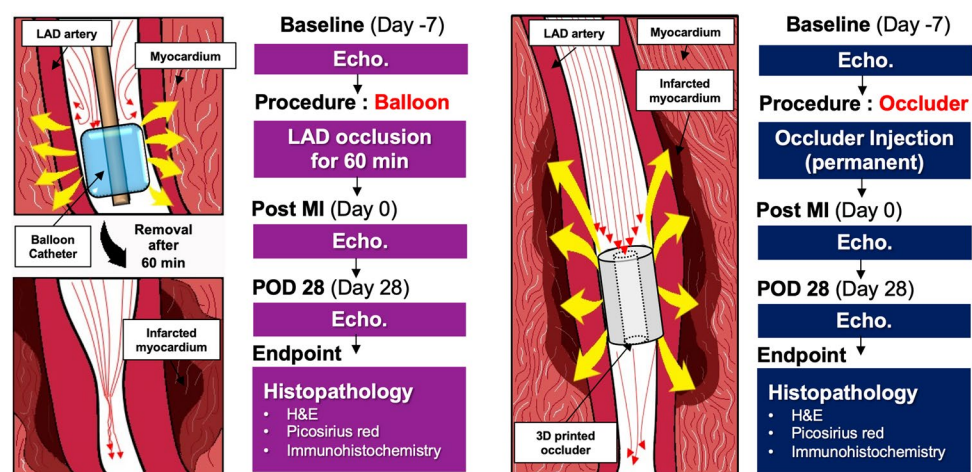
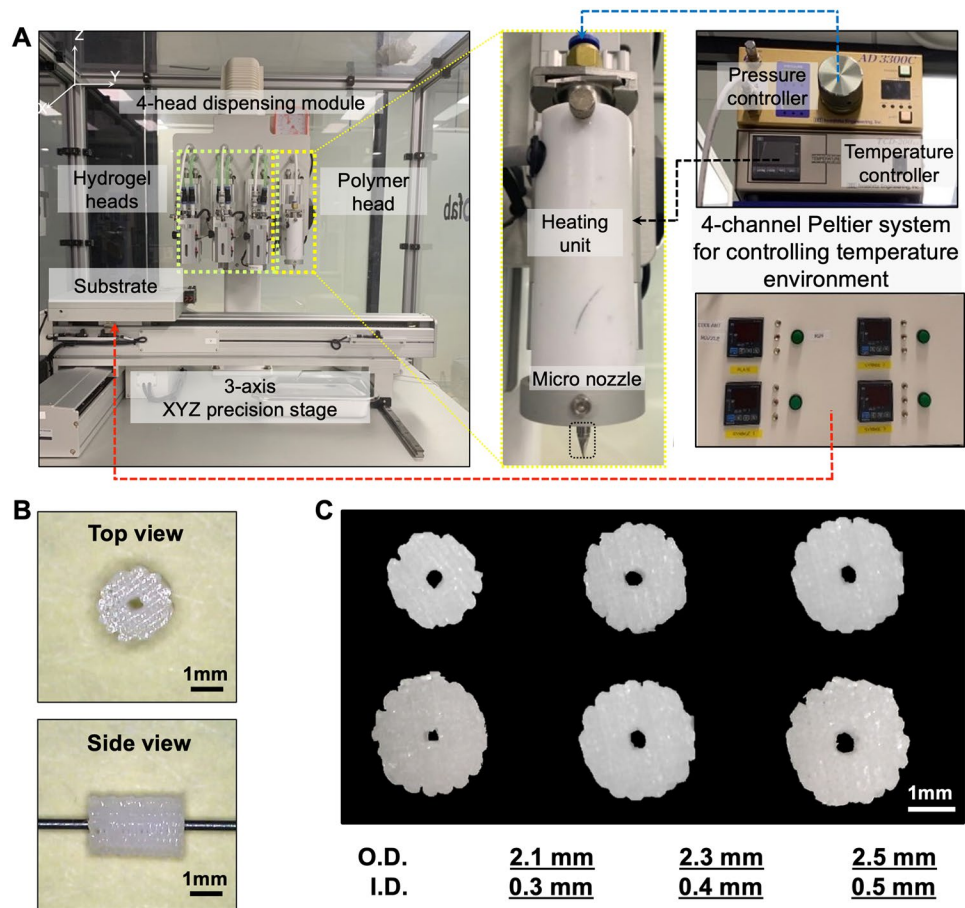


Fig. 2 Customized occluder fabricated using 3D-printing system that can induce partial blockage of the LAD artery. **a** Images of the 3D-printing system, **b** front and side views of the occluder inserted into the guide wire, and **c** occluders that are size-controllable by changing design parameters (O.D.—outer diameter, I.D.—inner diameter)



into the LCA under fluoroscopic guidance by using a mobile fluoroscope (BV Pulsera, Philips Medical Systems, Andover, MA, USA). The catheter was located at the mid-LAD artery and the balloon (3.0×20 mm, Terumo Co., Tokyo, Japan) was inflated for a complete blockage of blood flow. The occlusion was continued for 60 min with the condition of 7–8 atmospheres. As a pre-treatment, lidocaine (10 mg/kg) was injected intravenously to prevent ventricular fibrillation [12], and diclofenac sodium (2 mL, Dong Kwang Pharm Co., Republic of Korea) was intramuscularly injected pre- and postoperatively to reduce pain.

Induction of MI using the proposed method (occluder)

The luminal diameter of the LAD artery was measured from the baseline to the middle LAD position using an angiographic system (Supplementary Fig. S1), and a properly sized occluder was selected for the delivery. After the delivery of the occluder at the mid-LAD artery of the pig heart, the guidewire was removed.

Transthoracic echocardiography

The cardiac functions of swine were monitored at the baseline (before the procedure), post-MI (days 7–14), and 28 days postoperative day (POD) (from the post-MI) using two-dimensional transthoracic echocardiography (Vivid S5, GE medical systems, Vingmed Ultrasound, Horten, Norway). Parasternal long- and short-axis images were obtained by placing the transducer at the right parasternal echo window with subjects slightly tilted to the right side. Apical view images were also obtained by placing the transducer at the lower right chest with subjects tilted more to the right side. The functions of the left ventricle (LV) were measured by volumetric calculation through the biplane method of disk summation (modified Simpson's method). LV volumes were measured from the apical 4- and 2-chamber views by tracing the interface between the compacted layer of the endocardium and blood. All apical views were obtained without foreshortening of the LV and without losing the tracing of any LV segments. Based on the modified Simpson's method, left ventricular ejection fraction (LVEF), LV end-systolic volume (LVESV), and LV end-diastolic volume (LVEDV) were measured [14].

Triphenyltetrazolium chloride staining

Triphenyltetrazolium chloride (TTC) staining (Sigma-Aldrich, USA) was conducted to identify the area of necrosis in the infarcted myocardium. After completing the experiment, the isolated heart was vertically sliced from the apex to the LV at every 2 cm in thickness. Then, the tissue sections were incubated in 1% TTC diluted in PBS (pH 7.4) for 15 min at 37 °C.

Histology and immunohistochemistry

Isolated hearts were collected and fixed in 4% paraformaldehyde for 48 h and were sectioned (4 µm) in thickness by using a microtome (Accu-Cut[®], SRM[™] 200, Sakura[®], CA, USA). Hematoxylin (Muto, Japan) and eosin (Merk, USA) (H&E) staining and picrosirius red staining (Abcam, USA) were performed to investigate the area of ischemic myocardium and collagen deposition, representing scar formation. Immunohistochemistry was performed by using anti-hypoxia-inducible factor 1- α (HIF-1 α) (1:100; Abcam, USA) as the primary antibody and goat anti-mouse IgG H&L (1:1,000; Abcam, USA) as the secondary antibody. 3–3'-Diaminobenzidine (DAB) was detected using a peroxidase substrate kit (Vector Laboratories, USA) and subsequently imaged with an upright microscope (Eclipse 80i; Nikon, Tokyo, Japan). In order to evaluate the quantitative collagen deposition, the samples stained with picrosirius red solution ($n=3$ in the normal region; $n=8$ in the infarct region induced by the occluder) were analyzed with *ImageJ* (version 1.48v; National Institutes of Health, USA). Two independent pathologists evaluated the immunohistochemically stained sections through blind testing and scored the stained images for assessing HIF-1 α intensity. The immunoreactive score (IRS) was selected as the system of scoring and was calculated by multiplying the intensity of stained cells with the percentage of positively stained cells ($n=3$ in the normal region; $n=8$ in the infarct region induced by the occluder) [15–17].

Statistical analysis

We used the Statistical Package *GraphPad Prism 6.0* (GraphPad Software, La Jolla, CA, USA) for all analyses. All numerical variables were presented as mean \pm standard deviation (SD) and were compared by an independent sample *t*-test or log-rank test. A $p < 0.05$ was considered as statistically significant.

Results

Induction of MI using the 3D-printed occluder

The customized occluder (Fig. 2b and 2c) was fabricated based on the size of the middle LAD artery and was inserted

into the carotid artery through a 9-F introducer sheath and a 9-F guiding catheter (Fig. 3a and 3b). In brief, the tip of a guide wire that was fixed at the top of the catheter was inserted into the hole of the occluder to be placed properly in the LAD artery (Fig. 3c and 3d). Once the catheter was inserted into the mid-LAD position, it was immediately removed with only the occluder left inside the LAD artery (Fig. 3e). The customized occluder remained at the site of the LAD without any positional inaccuracy for 28 days. The left coronary angiogram showed partial blood flow through the occluder, highlighting the increased survival rate of swine during the experimental period (Fig. 3f).

Profound effect of the occluder on creating stable MI condition in swine models

During the observation period, collaterals and neovascularization due to 3DBO occlusion were not detected in coronary angiography. In order to validate the occurrence of MI in the swine model by using 3DBO, echocardiography of the balloon method was used as a control. From the baseline to post-MI, LVEF significantly decreased in both groups ((62.37 \pm 2.77)% to (47.49 \pm 3.44)% for balloon and (61.68 \pm 2.30)% to (41.23 \pm 6.16)% for occluder). Although the LVEF decline was observed in the acute phase from baseline to post-MI, the balloon group failed to demonstrate a consistent decline in LVEF to the later phase (POD 28) ((47.49 \pm 3.44)% to (55.44 \pm 2.77)%). In contrast, the occluder induced a gradual and consistent LVEF decline throughout the experimental timeline, thereby maintaining a stable and consistent swine MI model ((41.23 \pm 6.16)% to (39.49 \pm 4.19)%) (Fig. 4). In addition, measured LVEDV and LVESV during the 28 days of follow-up showed a gradual increase, suggesting the effectiveness of the occluder in inducing a stable MI (Supplementary Figs. S2 and S3).

Functional evaluation post-myocardial infarction

TTC staining displayed a prominent white area of infarction in the apex and LV anterior wall (Fig. 5a). Compared to the normal region, H&E staining showed a loss of normal architecture and morphology of myocytes in the LV myocardium (Fig. 5b). Picrosirius red staining confirmed a significantly increased area of collagen deposition in the surrounding ischemic area, compared to the normal myocardium ((42.01 \pm 1.76)% vs. (1.83 \pm 0.51)%). HIF-1 α was only barely expressed in the normal region, whereas the occluder group clearly expressed HIF-1 α in the ischemic myocardium (Fig. 5b). The quantified HIF-1 α intensity score of the occluder group demonstrated significantly higher values as compared to the score obtained from the normal region (6.50 \pm 2.50 vs. 0.67 \pm 0.47) (Fig. 5c). The infarct size of the tissues obtained from the occluder group was approximately double the size of the balloon group on

Fig. 3 Angiographic imaging depicting induction of heart failure through occluder placement. **a** Swine placed on the cardiac fluoroscopic table in supine position. **b** Angiogram showing left anterior descending artery (LAD, white arrow) and left anterior circumflex artery (LCX, red arrow). **c** Guidewire (GW, white arrow) injection toward LAD artery. **d** Occluder placement in distal position to mid LAD (white arrow) by using a catheter. **e** Extraction of a GW for leaving the occluder in the LAD artery. **f** Partial blood blockage by occluder placement

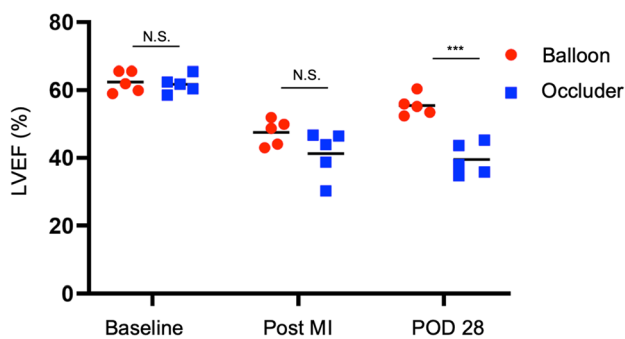
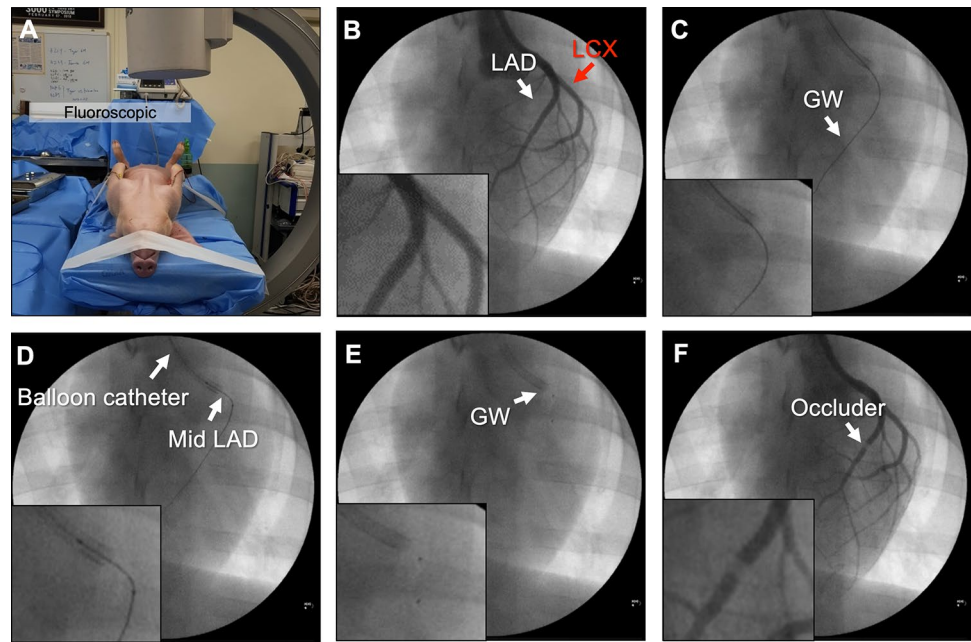


Fig. 4 Echocardiography results after MI induction (left ventricular ejection fraction (LVEF); $n=5$) (** $p < 0.0001$)

POD 28, indicating the reliability of the suggested method for maintaining the injury. This trend was similar to that of results from echocardiography (Fig. 5d).

Increased survival rate with the use of occluders

The occluder group exhibited an 88% survival rate in the swine MI model as compared to the balloon group, which showed a 50% survival rate. This highlighted that our strategy of fabricating custom-made, anatomically relevant occluders holds the potential to improve the survival rate for swine models during the post-surgical period. Hence, the suggested strategy of using occluders to induce MI in swine could be a promising approach to overcoming the associated drawbacks of existing conventional methods (Fig. 6).

Discussion

MI models, typically induced in large animals, consist of invasive and non-invasive methods. In general, invasive methods (e.g., thoracotomy) cause a non-physiological and hostile environment (e.g., pericardial injury, inflammation, and pneumothorax) in the heart [18, 19]. Non-invasive closed-chest methods (e.g., catheter-based approaches) can be used to induce acute MI through a balloon catheter-occlusion inside the LAD artery for 50 to 60 min. This procedure results in microcirculatory reperfusion injury (RI), obstructing microvasculature and causing MI [20]. However, this method increases mortality and causes an uncontrollable range of myocardial ischemia during the procedure [21]. Although such limitations might be solved with the use of a defibrillator, anatomical and physiological variations in animal models, as well as the defibrillator's collateral effects, increase LVEF, thus interfering in the extracted experimental results [22, 23]. In addition, the survival rate is significantly reduced over time, and it is difficult to maintain the cardiac dysfunction of pigs over a longer time period (i.e., 28–56 days). Therefore, in this study, we did not use the conventional balloon system, but designed various outer and inner diameters of the occluder to investigate the proper sizes and conditions for the partial blockage of the coronary artery, resulting in an increase in the survival rate of pigs with the reliable induction of the injury.

The use of 3D-printing technology in medicine is rapidly increasing, and it is widely used in the development of customized implants, pre-surgery 3D modelling, prosthetics, and stents [24–26]. This present study showcases the feasibility of 3D-printing technology as an alternative

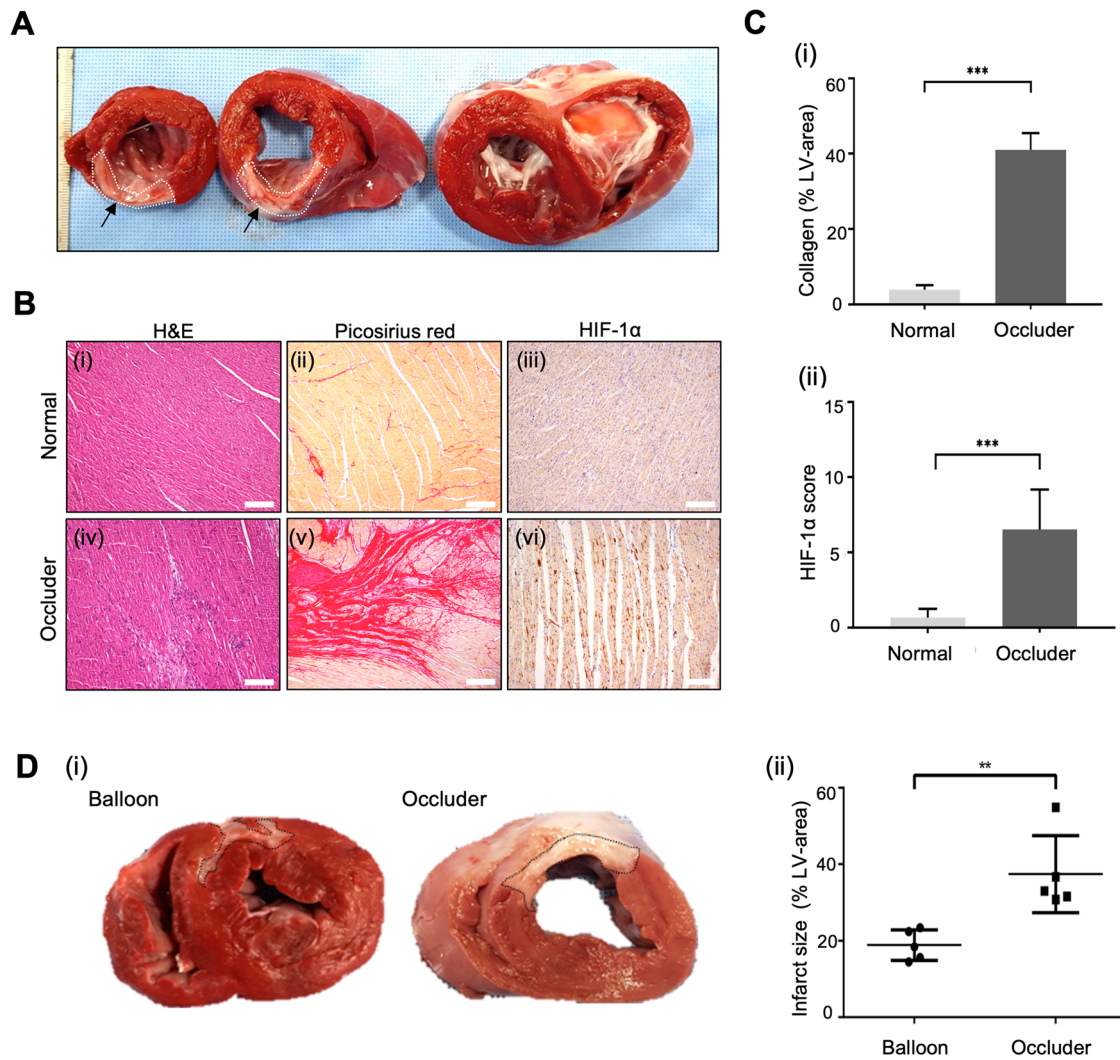


Fig. 5 Histopathological analysis for the infarcted tissue by post-occlusion after 28 days. **a** Representative images of cross-sectional tissue slices of the occluder group stained by triphenyltetrazolium chloride (TTC) at POD 28 (arrow: infarct region). **b** Histological analysis of normal and occluder groups, observed by (i, iv) hematoxylin and eosin (H&E) staining, (ii, v) picrosirius red staining, and (iii,

vi) immunohistochemical expression of hypoxia inducible factor-1 alpha (HIF-1 α) (Bar: 100 μ m). **c** Quantitative assessments of the tissues by measuring (i) the area of collagen deposition and (ii) HIF-1 α score (** $p < 0.0001$). **d** (i) TTC staining of the balloon and occluder groups at POD 28 and (ii) its quantitative results (** $p < 0.001$)

and promising way to fabricate target specific occluders for inducing MI in a single step, in a minimally invasive procedure, in order to overcome the associated drawbacks of existing methods. Our results demonstrate that using occluders to induce MI in the LAD artery attenuated ischemic injury of the LV, with a significant reduction in post-infarct cardiac remodeling and the preservation of LV functions [27].

No inflammatory response or immune rejection was observed during the surgical procedure, which could be attributed to the use of biocompatible PCL, a widely available material used for various clinical applications [28]. MI is caused mainly by chronic stenosis of coronary arteries and arterial thrombus formation that creates an insufficient

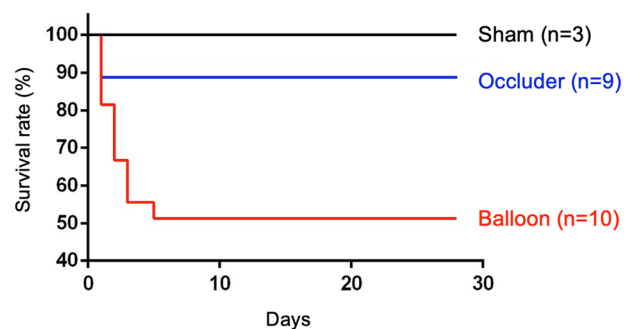


Fig. 6 Significant improvement of survival rate in the occluder group on POD 28

oxygen supply in the tissue [29]. A decreased oxygen level leads to reduced mitochondrial respiration and oxidative metabolism that further cause cell death [30]. As a critical transcriptional regulator of hypoxia, HIF-1 α is severely expressed under hypoxic and ischemic conditions [31, 32]. Our method also can reduce the time needed for induction and does not require waiting for 60–90 min for balloon removal.

Taken together, the results suggest that the occluder facilitated the induction of an effective MI condition in the swine model by conserving the physiological environment due to blood flow through the hole of the occluder. Thus, the study portrayed the fabrication of a custom-made occluder that aids in the induction of MI in swine models and demonstrated an improvement of up to 38% in the survival rate when compared to existing methods, thereby suggesting it to be an alternative approach for clinical application. Although the suggested method showed significance in reducing mortality and promoting the effectiveness of creating reliable animal models, there are several challenges to overcome. We designed various outer and inner diameters of the occluder and investigated proper sizes and conditions; however, all design criteria, such as surface roughness and the roundness of occluders, could not be standardized, resulting in remaining partial blood flow at the periphery of the LAD artery. In addition, the quantitative analysis of cardiac biomarkers enables the control and estimation of the infarct size. Therefore, cardiac biochemical markers such as troponin I, myoglobin, total creatine kinase, and lactate dehydrogenase should be assessed in a follow-up study.

Conclusions

The present study demonstrates that a 3D-printed occluder produces a stable, consistent, and reproducible MI model by showing a prominent infarcted region, consistent and long-lasting LV dysfunction, and an improved survival rate. When compared with the limitations of conventional methods with a 50% survival rate, our strategy shows an improvement with an 88% survival rate. In conclusion, the occluder fabricated using a printing technology could be a promising strategy for inducing MI and providing a cardiac research platform for large animal studies.

Supplementary Information The online version contains supplementary material available at <https://doi.org/10.1007/s42242-021-00145-4>.

Acknowledgements This research was supported by the Bio & Medical Technology Development Program and Basic Science Research Program through the National Research Foundation (NRF), funded by the Korean government (MSIT) (No. 2018M3A9E2024584) and the Ministry of Trade, Industry and Energy (MOTIE) and Korea Institute

for Advancement of Technology (KIAT) through the International Cooperative R&D program (No. P0011282).

Author contributions HBK, HP, DSS, MK, YA, MHJ, and YJH conducted all animal experiments and analyzed experimental results. SJ and JJ developed and fabricated a 3D-printed occluder and analyzed experimental results. HBK and SJ were involved in writing-original draft and visualization. SD was involved in writing-review and editing. JJ and YJH were involved in conceptualization, writing-original draft, review and editing, and contributed to supervision and funding acquisition.

Declarations

Conflict of interest The authors declare that there is no conflict of interest.

Ethical approval All institutional and national guidelines for the care and use of laboratory animals were followed.

References

1. Sanchis-Gomar F, Perez-Quilis C et al (2016) Epidemiology of coronary heart disease and acute coronary syndrome. *Ann Transl Med* 4(13):7. <https://doi.org/10.21037/atm.2016.06.33>
2. Mozaffarian D, Benjamin EJ, Go AS et al (2016) Heart disease and stroke statistics—2016 update. *Circulation* 133(4):e38–e360. <https://doi.org/10.1161/CIR.0000000000000350>
3. Rodrigues M, Silva A, Aguas A et al (2020) The coronary circulation of the pig heart: comparison with the human heart. *Eur J of Anat* 9(2):67–87
4. Sun S, Guo T (2009) Model establishment of acute myocardium infarction induced by coronary occlusion versus balloon occlusion in miniature pigs. *J Clin Rehabil Tissue Eng Res* 13:9913–9916. <https://doi.org/10.3969/j.issn.1673-8225.2009.50.023>
5. Tang YP, Liu Y, Fan YJ et al (2018) To develop a novel animal model of myocardial infarction: a research imperative. *AMEM* 1(1):36–39. <https://doi.org/10.1002/ame2.12010>
6. Krombach GA, Kinzel S, Mahnken AH et al (2005) Minimally invasive close-chest method for creating reperfused or occlusive myocardial infarction in swine. *Invest Radiol* 40(1):14–18
7. Biondi-Zoccai G, De Falco E, Peruzzi M et al (2013) A novel closed-chest porcine model of chronic ischemic heart failure suitable for experimental research in cardiovascular disease. *Biomed Res Int*. <https://doi.org/10.1155/2013/410631>
8. Bergely JL, Nocella K, McCallum JD (1982) Acute coronary artery occlusion-reperfusion-induced arrhythmias in rats, dogs and pigs: antiarrhythmic evaluation of quinidine, procainamide and lidocaine. *Eur J Pharmacol* 81(2):205–216. [https://doi.org/10.1016/0014-2999\(82\)90438-1](https://doi.org/10.1016/0014-2999(82)90438-1)
9. Hawk C, Leary S, Morris T (2005) American college of laboratory animal medicine, european college of laboratory animal medicine. *Formulary for laboratory animals*, 3rd edn. Blackwell Pub, Ames, Iowa
10. Ye L, Chang YH, Xiong Q et al (2014) Cardiac repair in a porcine model of acute myocardial infarction with human induced pluripotent stem cell-derived cardiovascular cells. *Cell Stem Cell* 15(6):750–761. <https://doi.org/10.1016/j.stem.2014.11.009>
11. Munz MR, Faria MA, Monteiro JR et al (2011) Surgical porcine myocardial infarction model through permanent coronary occlusion. *Comp Med* 61(5):445–452

12. Jang J, Park HJ, Kim SW et al (2017) 3D printed complex tissue construct using stem cell-laden decellularized extracellular matrix bioinks for cardiac repair. *Biomaterials* 112:264–274. <https://doi.org/10.1016/j.biomaterials.2016.10.026>
13. Kim BS, Das S, Jang J et al (2020) Decellularized extracellular matrix-based bioinks for engineering tissue- and organ-specific microenvironments. *Chem Rev* 120(19):10608–10661. <https://doi.org/10.1021/acs.chemrev.9b00808>
14. Schiller NB, Shah PM, Crawford M et al (1989) Recommendations for quantitation of the left ventricle by two-dimensional echocardiography. *J Am Soc Echocardiogr* 2(5):358–367. [https://doi.org/10.1016/S0894-7317\(89\)80014-8](https://doi.org/10.1016/S0894-7317(89)80014-8)
15. Eckert AW, Schutze A, Lautner MH et al (2010) HIF-1 α is a prognostic marker in oral squamous cell carcinomas. *Int J Biol Markers* 25(2):87–92. <https://doi.org/10.1089/hyb.2009.0115.MAb>
16. Colbert LE, Fisher SB, Balci S et al (2015) High nuclear hypoxia-inducible factor 1 α expression is a predictor of distant recurrence in patients with resected pancreatic adenocarcinoma. *Int J Radiat Oncol Biol Phys* 91(3):631–639. <https://doi.org/10.1016/j.ijrobp.2014.11.004>
17. Stavrou S, Gratz M, Tremmel E et al (2018) TAAR1 induces a disturbed GSK3 β phosphorylation in recurrent miscarriages through the ODC. *Endocr Connect* 7(2):372–384. <https://doi.org/10.1530/ec-17-0272>
18. Hosenpud JD, Yung N, Morton MJ (1983) Left ventricular pressure-volume relations shift to the left after long-term loss of pericardial restraint. *Circulation* 68(1):155–163. <https://doi.org/10.1161/01.CIR.68.1.155>
19. Reffelmann T, Sensebat O, Birnbaum Y et al (2004) A novel minimal-invasive model of chronic myocardial infarction in swine. *Coron Artery Dis* 15(1):7–12. <https://doi.org/10.1097/00019501-200402000-00002>
20. Fröhlich GM, Meier P, White SK et al (2013) Myocardial reperfusion injury: looking beyond primary PCI. *Eur Heart J* 34(23):1714–1722. <https://doi.org/10.1093/eurheartj/ehd090>
21. Schwartz LM, Lagranha CJ (2006) Ischemic postconditioning during reperfusion activates Akt and ERK without protecting against lethal myocardial ischemia-reperfusion injury in pigs. *Am J Physiol-Heart C* 290(3):H1011–H1018. <https://doi.org/10.1152/ajpheart.00864.2005>
22. Rissanen TT, Nurro J, Halonen PJ et al (2013) The bottleneck stent model for chronic myocardial ischemia and heart failure in pigs. *Am J Physiol-Heart C* 305(9):H1297–H1308. <https://doi.org/10.1152/ajpheart.00561.2013>
23. Radke PW, Heintl-Green A, Frass OM et al (2006) Evaluation of the porcine ameroid constrictor model of myocardial ischemia for therapeutic angiogenesis studies. *Endothelium* 13(1):25–33. <https://doi.org/10.1080/10623320600660128>
24. Bose S, Vahabzadeh S, Bandyopadhyay A (2013) Bone tissue engineering using 3D printing. *Mater Today* 16(12):496–504. <https://doi.org/10.1016/j.mattod.2013.11.017>
25. Park SA, Lee SJ, Lim KS et al (2015) In vivo evaluation and characterization of a bio-absorbable drug-coated stent fabricated using a 3D-printing system. *Mater Lett* 141:355–358. <https://doi.org/10.1016/j.matlet.2014.11.119>
26. Morrison RJ, Kashlan KN, Flanagan CL et al (2015) Regulatory considerations in the design and manufacturing of implantable 3D-printed medical devices. *Clin Transl Sci* 8(5):594–600. <https://doi.org/10.1111/cts.12315>
27. Kim HK, Jeong MH, Ahn Y et al (2017) Relationship between time to treatment and mortality among patients undergoing primary percutaneous coronary intervention according to Korea acute myocardial infarction registry. *J Cardiol* 69(1):377–382. <https://doi.org/10.1016/j.jjcc.2016.09.002>
28. Nair LS, Laurencin CT (2007) Biodegradable polymers as biomaterials. *Prog Polym Sci* 32(8–9):762–798. <https://doi.org/10.1016/j.progpolymsci.2007.05.017>
29. Berne RM (1963) Cardiac nucleotides in hypoxia: possible role in regulation of coronary blood flow. *Am J Physiol Content* 204(2):317–322. <https://doi.org/10.1152/ajplegacy.1963.204.2.317>
30. Reimer KA, Lowe JE, Rasmussen MM et al (1977) The wavefront phenomenon of ischemic cell death. 1. Myocardial infarct size vs duration of coronary occlusion in dogs. *Circulation* 56(5):786–794. <https://doi.org/10.1161/01.CIR.56.5.786>
31. Lee SH, Wolf PL, Escudero R et al (2000) Early expression of angiogenesis factors in acute myocardial ischemia and infarction. *N Engl J Med* 342(9):626–633. <https://doi.org/10.1056/NEJM200003023420904>
32. Tekin D, Dursun AD, Xi L (2010) Hypoxia inducible factor 1 (HIF-1) and cardioprotection. *Acta Pharmacol Sin* 31(9):1085–1094. <https://doi.org/10.1038/aps.2010.132>